Polymer Degradation and Stability 96 (2011) 919–928

Contents lists available at ScienceDirect

Polymer Degradation and Stability

journal homepage: www.elsevier.com/locate/polydegstab

Kinetics of abiotic and biotic degradability of low-density polyethylene containing prodegradant additives and its effect on the growth of microbial communities

Ignacy Jakubowicz [a,*], Nazdaneh Yarahmadi [b], Veronica Arthurson [c]

[a] SP Technical Research Institute of Sweden, Sweden
[b] Carmel Pharma AB, Sweden
[c] SLU – the Swedish University of Agricultural Sciences, Sweden

ARTICLE INFO

Article history:
Received 21 December 2010
Received in revised form
20 January 2011
Accepted 28 January 2011

Keywords:
Degradable polyethylene
Accelerated aging
Biodegradation
PCR (polymerase chain reaction)
TRF (terminal restriction fragments)
T-RFLP (terminal-restriction fragment length polymorphism)

ABSTRACT

The kinetics of abiotic oxidation in the dark and the kinetics of biological mineralization in soil and in a compost environment of thermally oxidized LDPE were studied. It was demonstrated that different activation energies are obtained for the thermal oxidation, depending on the composition of the materials. Significantly higher levels of biodegradability have been obtained in a soil environment at 23 °C compared with the compost environment at 58 °C. After two years of mineralization, 91% conversion to carbon dioxide was obtained in the soil test, compared with 43% in the compost test. The differences between fungal, archaeal and bacterial community structures in soil and compost after 607 days of biodegradability assay were mapped out. It was found that the most dominant bacterial and fungal terminal restriction fragments (TRFs) in the compost containing the test material are significantly different from the TRFs in the other environments.

1. Introduction

Biodegradable plastics are a new generation of polymers emerging on the global market. Their use is predicted to increase because of an expanding range of potential applications driven by the growing use of plastics in packaging. Synthetic polymers are normally not biodegradable because of their hydrophobic nature, high molecular weight and the absence of functional groups that can interact with microorganisms. However, when such polymers are oxidized and degraded into low molecular mass species, they can be assimilated by microorganisms [1,2]. This means that oxo-biodegradation is a two-step process where the kinetics of abiotic oxidation is controlled by the type and amount of antioxidant and prodegradant systems present while the rate of biological degradation depends on the chemical composition of the oxidized material and the biological environment. Various types of degradation of polymers such as photo-oxidative, thermal, ozone-induced, catalytic and biological are extensively discussed in the review article by Singh and Sharma [3].

Evaluation of abiotic degradability sometimes requires use of accelerated tests because the natural tests may take a long time to produce the desired degradation level. To allow extrapolation of short-time data to predict long-term performance, an appropriate curve must be drawn through the short-term values obtained at elevated temperatures. The most common technique is a linear extrapolation following the Arrhenius relationship. However, degradation is caused by a number of different mechanisms for a given case; although some or all may follow the Arrhenius relation, there is no guarantee that the overall behaviour is of an Arrhenius form. Non-Arrhenius behaviour in accelerated aging is clearly demonstrated by Celina et al. [4].

Recently, many efforts have focused on the role of various microorganisms in biological decomposition of oxidized polyolefins, especially in environments simulating soil conditions (temperatures 25–30 °C). It has been shown that various bacteria are able to utilize oxidized PE as a substrate [5,6]. In many studies, fungi were considered for the degradation of LDPE because of their ability to form hydrophobic proteins that can adhere to the surface of PE [7,8]. It has also been shown by incubating oxidized PE with fungal strains previously isolated from soil [9] or from aerobically aged municipal landfill [10] that these fungi could degrade PE by the formation of a biofilm on the surface of the materials.

* Corresponding author. Tel.: +46 105165305; fax: +46 33103388.
E-mail address: ignacy.jakubowicz@sp.se (I. Jakubowicz).

0141-3910/$ – see front matter © 2011 Elsevier Ltd. All rights reserved.
doi:10.1016/j.polymdegradstab.2011.01.031

Despite these interesting results, two important questions remain unanswered. The first one is associated with methods used to assess the biodegradation level. Under aerobic conditions, carbon substrates can be converted both to carbon dioxide and new biomass. Normally, standardized test methods are based only on the determination of evolved carbon dioxide. This can, however, lead to underestimation of biodegradation levels if production of new biomass is significant. Chiellini et al. [11] reported the relationship between the free-energy content of a carbon substrate and its propensity for conversion to new microbial biomass rather than mineralization to CO_2.

The second question regards the time scale over which oxo-biodegradable (OBD) materials degrade and the extent to which they are biodegradable. Concerns have been raised that small plastic fragments cannot be colonized and assimilated by microbes and, consequently, the particles of plastic may be ingested by invertebrates, birds, animals or fish [12]. The risk of plastic fragments that remain in the soil is therefore an area of uncertainty because there are few scientific papers that deal with long-term biodegradability. The DEFRA report refers to a study conducted by Feuilloley et al., who showed a biodegradation of about 15% after 350 days of incubation. Husarova et al. [13] reported that after more than 460 days in soil, the final values of carbon mineralized, measured as evolved CO_2, were 13–16% while Fontanella et al. [5] measured 12% at the most after 352 days of incubation in soil. Chiellini et al. [14] performed a soil burial test for 85 weeks (600 days) and reached 63% biodegradation, adding some water and fresh soil inoculums after five months of incubation. In our earlier investigation [15], oxidized LDPE samples appeared to undergo biodegradation in a compost environment, reaching a mineralization level above 60% after 200 days.

The current study highlights the kinetics of abiotic and biotic degradation of LDPE film intended to remain in or on the soil after use and to undergo biodegradation. It also brings some light to the questions of conversion to carbon dioxide vs. new biomass, as well as the question of recalcitrant plastic particles. Special focus was directed towards comparison between the rates of biodegradability in compost and soil. In most investigations dealing with microorganisms in mineralization tests, some specific, isolated microorganisms were used to study biodegradability of PE. In our investigation, an important part of the study was instead a thorough characterization of the microbial communities that could be found in soil and in the compost environment after a very long mineralization period.

2. Experimental

2.1. Material

15-μm thick LDPE film containing a prodegradant system designated “P-Life”, which is based on a manganese salt, was kindly supplied by P-Life Japan Inc. The film was blown and transparent.

2.2. Abiotic degradability

Thermo-oxidative degradation of the film was performed in heating cabinets with low, laminar air flow at various temperatures, viz., 75, 65, 55 and 40 ± 1 °C. In addition to that, the material was also tested after keeping in standard atmosphere (23 °C, 50% RH). After various periods, one set of the test samples was used for the measurements of elongation at break. At the end of the test, size exclusion chromatography (SEC) analyses were performed.

2.3. Tensile testing

Tensile tests were performed using an Instron 5566 Universal Testing Machine equipped with an Instron Static Load Cell ±100 N and a video extensiometer. The crosshead speed was set to 100 mm/min. Conditioning and testing were performed at standard atmosphere (23 ± 2 °C and 50 ± 10% RH). The tensile test results are reported as the arithmetic mean of 10 test samples per series.

2.4. Molecular weight

Measurements of molecular weight of the abiotically degraded material were performed using SEC.

The molecular weight was determined using a high temperature Waters Alliance GPCV 2000 chromatograph equipped with two Shodex packed columns for HPLC and one Waters styragel HT 6E column. 1,2,4-Trichlorobenzene at a concentration of 1 g/l was used as the solvent at 135 °C, with a dissolving time of 16 h. Solutions of polystyrene standards were used for the calibration.

2.5. Biodegradability test

The ultimate biodegradability of the thermally degraded material was examined under optimal conditions simulating the soil environment at room temperature and in parallel with that in mature compost at 58 °C. A method involving analysis of evolved carbon dioxide was applied using a Maihak S710 analyzer equipped with Multor NDIR detector with measurements every 14 h. Air that was free of carbon dioxide was passed at the rate of 300 ml/min through the mineralization vessels. Three parallel vessels (6l desiccators) were used for the test of oxidized material. Cellulose (Merck, microcrystalline powder for thin layer chromatography, Avicel, 11.0 g, containing 44.4% C) was used as the positive reference material in three vessels. The cellulose was added at two different occasions in soil and three different occasions in compost because of the fast bioassimilation compared with the total test duration. Each time, eventually, the cellulose was totally converted to carbon dioxide. Three vessels were also used as blanks, containing either the soil or the compost only but no test material.

2.5.1. Biodegradability testing in soil

The soil environment was simulated using a mixture of equal parts by volume of mature compost, plant soil and Vermiculite of concrete type. Vermiculite was added to create a larger volume and to improve the signal-to-noise ratio. The total weight of the soil mixture was 1239 g including water, of which 447 g was dry matter. The pH of the soil mixture was 7.5. About 13 g of previously oxidized film was added to each vessel. The test was performed in principle according to ISO 17556 at room temperature (23 ± 2 °C).

2.5.2. Biodegradability test in compost

Industrial compost was simulated by a mixture consisting of 50% (by volume) mature compost and 50% expanded Vermiculite of concrete type as structural material. The total weight of the compost mixture was 1239 g including water, of which 439 g was dry matter. The pH of the compost mixture was 7.9. About 12.5 g of previously oxidized film was added to each vessel. The test was performed in accordance with ISO 14855-1. Before adding the test material, the compost mixture was pre-incubated at 58 ± 2 °C for five days to reduce the compost activity enough for the IR detector to be able to measure the evolved carbon dioxide. Three parallel composting vessels (6l desiccators) were used for the oxidized material. However, after about two months one vessel was broken, thus only two parallel vessels were used thereafter.

2.6. Analysis of bacterial, archaeal and fungal communities

To obtain a basis for the assessment of possible differences between communities of soil and compost microorganisms, four

different samples were subjected to analyses of bacterial, archaeal and fungal communities as described below. The samples of soil and compost were taken after 607 days of mineralization as follows:

A. Soil containing residues of the test material (mineralization level: 79%);
B. Soil containing residues of the reference material (cellulose) (mineralization level: 92%);
C. Compost containing residues of the test material (mineralization level: 43%);
D. Compost containing residues of the reference material (cellulose) (mineralization level: 104%).

A–D are referred to as environments in this paper.

The methods used in the present work identify the **dominant** groups within microbial communities and consequently several species that are not among the most dominant members were not detected here. The main goal was to get a broad overview of the differences in microbial community compositions between environments, thus not all microorganisms present in each community were identified.

2.6.1. DNA extraction

Genomic DNA was extracted from 500 mg of four subsamples of each of the four environments (16 extractions in total) using a FastDNA kit (Bio 101, Carlsbad, CA), according to the manufacturer's recommendations in combination with an extra washing step. The isolated DNA was immediately stored at −20 °C until use and DNA concentrations were determined using a spectrophotometer (Ultrospec 1100 pro; GE Healthcare).

2.6.2. PCR (polymerase chain reaction) and T-RFLP (terminal-restriction fragment length polymorphism) analysis of bacterial, archaeal and fungal genes

For T-RFLP analysis of 16S rRNA bacterial gene fragments in all samples, the universal primers 926r (5′-CCGTCAATTCCTTTRAGTTT-3′) [16] and fD1 (5′-AGAGTTTGATCCTGGCTCAG-3′) [17] were used. For analysis of archaeal and fungal populations, the primer pairs A571F-FAM [20] and UA1204r [20], and ITS1-FAM [21] and ITS4 [21], respectively, were used. Moreover, the forward primers were ′-end-labelled with phosphoramidite fluorochrome 5-carboxy-fluorescein (5′6FAM). Amplification was performed in 50 μl reaction mixtures with 35 pmol of each primer, 2.5 U Taq DNA polymerase (Amersham Bioscience, NJ), 1× PCR buffer, 15 nmol dNTPs, ~25 ng of template DNA and sterile distilled water. Thermal cycling was conducted with a Gene Amp PCR system (model 9700; Applied Biosystems, Fremont, CA) for the bacterial amplification starting with a first denaturation step of 95 °C for 3 min, followed by 35 cycles comprising 40 s at 94 °C, 40 s at 55 °C and 1 min at 72 °C, and a final primer extension step at 72 °C for 7 min. The annealing temperatures were 59 °C and 60 °C for the primer pairs A571F/UA1204R and ITS1/ITS4, respectively, the rest of the reactions constituents and amplification conditions remaining the same. For each sample, 20 ng DNA of PCR products were mixed and incubated for 2 h at 37 °C in three separate restriction digestions with 5 U of HaeIII, HhaI or MspI for the bacteria, 5 U of TaqI, RsaI or NlaIII for the archaea and 5 U of MaeII, BfaI or BstNI (New England Biolabs) for the fungal DNA. In the HhaI, BstNI and TaqI digests, 5 μl of 0.1% BSA was added to the general mixtures.

The DNA fragments were separated using a capillary sequencer (ABI3700; Applied Biosystems). Prior to injection, 1.4 μl of the DNA sample was denatured in the presence of 10 μl Hi-Di™ formamide at 95 °C for 5 min and 0.04 μl GS ROX-500 size standard (Applied Biosystems) was added. Injection was performed electrokinetically at 10 kV for 50 s, followed by electrophoresis at 7.5 kV for 80 min.

The lengths and peak areas of the terminal restriction fragments (TRFs) were determined using Peak Scanner software (Applied Biosystems). Only TRFs in the range 50–500 bp of the total area were considered. The T-RFLP community structures produced by restriction digestion with HaeIII, TaqI and MaeII generated higher numbers of TRFs in the profiles than did community profiles generated with the other enzymes and were thus employed for diagrams and matching of sequences from clone libraries to corresponding TRFs. When comparing community profiles among treatments with non-metric multidimensional scaling (NMS) analyses, the patterns produced by all three restriction enzymes were used.

2.6.3. Construction of clone libraries

To identify individual TRFs in T-RFLP profiles, clone libraries were created using a mixture of the four DNA samples extracted from the compost and soil (environments C and A). Amplification of 16S rRNA genes from bacterial and archaeal populations and from the fungal region ITS-5.8S rDNA was carried out under the same conditions as described for T-RFLP, except that the fD1, A571F and ITS1 primers were unlabelled. The PCR products were processed on a gel (1% agarose), cloned into PCR®4-TOPO® plasmid vectors (Invitrogen, Carlsbad, CA) and transformed into chemocompetent TOP10 *Escherichia coli* cells, following the manufacturer's recommendations (Invitrogen). 3 ml cultures were prepared from each positive clone colony and the plasmid DNA was extracted using the QIAGEN Plasmid Miniprep kit (Qiagen). The M13f and M13r primers, provided by the miniprep kit manufacturer (Invitrogen) were used to amplify the inserts, followed by digestion with HaeIII, RsaI and BfaI (New England Biolabs) for 2 h at 37 °C. 10 ml of the generated restriction fragments were separated and evaluated by gel electrophoresis (1% agarose gels for 1.5 h at 70 V). The restriction profiles were visually evaluated and clones displaying similar patterns were assigned discrete operational taxonomic units (OTUs). Depending on the number of clones present in the groups, between one and four clones from each OTU were sequenced by Macrogen Inc. (Korea) using the T3 and T7 primers on an International 3730 XL automatic DNA sequencer (Applied Biosystems). In total, 102 clones from the bacterial clone libraries (compost and soil) were analyzed by RFLP and 24 unique restriction patterns were obtained. A total of 82 clones were subjected to sequencing, which resulted in the identification of 24 unique sequences. For the archaeal clone libraries, 40 clones were analyzed by RFLP, resulting in two unique restriction patterns, of which 10 clones were sequenced and two unique sequences identified. The fungal clone libraries showed eight unique RFLP patterns out of 124 examined clones, leading to sequencing of 29 clones and 10 unique sequences.

2.6.4. Coupling TRFs with sequences of cloned inserts and phylogenetic analysis

In silico digestion of the sequences with HaeIII (bacteria), TaqI (archaea) or MaeII (fungi) was performed, and the generated TRFs were compared with those generated in the T-RFLP analysis. Differences $\leq$ 3 bp were automatically considered to belong to the same OTU. Each cloned sequence contained terminal restriction sites for HaeIII (bacteria), TaqI (archaea) or MaeII (fungi) within the investigated part of the DNA region, and was linked to a corresponding TRF in the community structure (Figs. 5 and 6). To generate putative identities of the TRFs, the cloned sequences were subjected to similarity analyses using the Ribosomal Database Project (RDPII; http://rdp.cme.msu.edu/).

Sequences were aligned using CLUSTALW in the Mobyle package (mobyle.pasteur.fr/), followed by construction of Maximum-likelihood trees using PHYML 3.0 software. Closely related sequences

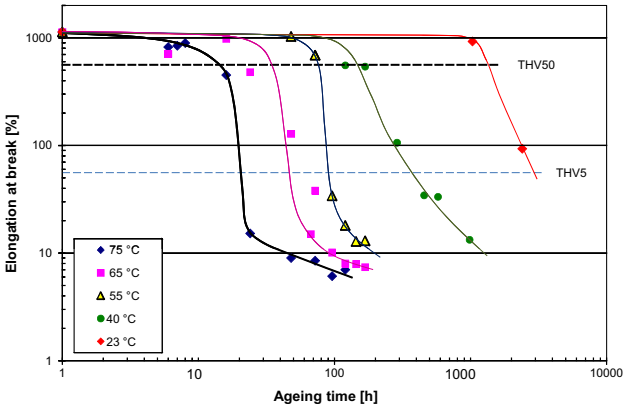

Fig. 1. Change in elongation at break as a function of exposure time in heating cabinets at various temperatures.

were used as references in the phylogenetic tree and the trees were edited and drawn using MEGA 4.0, and Adobe Illustrator CS4.

2.6.5. Statistical analysis

The T-RFLP data showing the bacterial, archaeal or fungal community structure was analyzed with the non-parametric ordination method non-metric multidimensional scaling (NMS) using PC-ORD v. 5.10 (MjM Software, Oregon, USA). Bray–Curtis distance measure was used to create distance matrices, based on arcsin transformed relative abundance values of TRFs obtained after cleavage with all three restriction enzymes for each microbial group and the pH values. The ordination was rotated using Varimax [22] to maximize variance of the different parameters included in the analysis. NMS ordination was performed with a random starting configuration, a maximum of 250 iterations and an instability criterion of 0,00001. Possible correlations between pH and community structures were evaluated and visualized as vectors in joint plots. Moreover, Mantel's test [23] with 999 Monte Carlo simulations was applied to determine relationships between pH and the bacterial, archaeal and fungal community structure, respectively, by correlating the dissimilarity matrices using PC-ORD v. 5.10.

Table 1
Molecular weight.

	Original	After 7 days at 65 °C	After 10 days at 65 °C
M_w	131,500	23,000	8800
M_n	18,300	2500	1700

2.6.6. Nucleotide sequence accession numbers

The nucleotide sequences of the clones have been deposited in GenBank under accession numbers HQ693485–HQ693523.

3. Results and discussion

3.1. Thermo-oxidative degradation

Lifetime prediction often requires extrapolation of accelerated aging data. Two threshold values are of great importance for oxo-biodegradable materials. The first one considers the time to create changes that have an immediate impact on properties that determine the service life of the material. In most cases, this time is defined as 50% deterioration of the elongation at break (THV50). The second value is connected to the extent of oxidative degradation sufficient to create low molecular mass species that can be assimilated by microorganisms. In the standard ASTM D 6954, this value is defined as $\leq$5% of the original elongation at break (THV5).

Therefore, in our investigation the exposure periods to achieve 50% and 5% of the original elongation at break were read off in Fig. 1 from the curves corresponding to heat aging at 75, 65, 55, 40 and 23 °C. These readings were then used to draw appropriate Arrhenius curves using the equation below:

$$\ln t = (E_a/R)\cdot 1/T + B$$

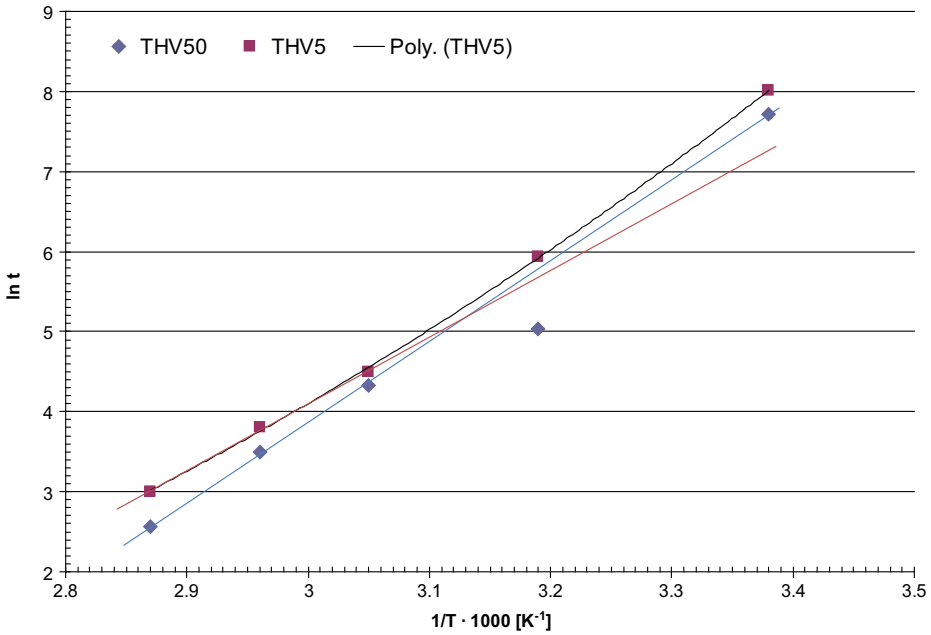

Fig. 2. Arrhenius plot using two threshold values viz. THV50 and THV5.

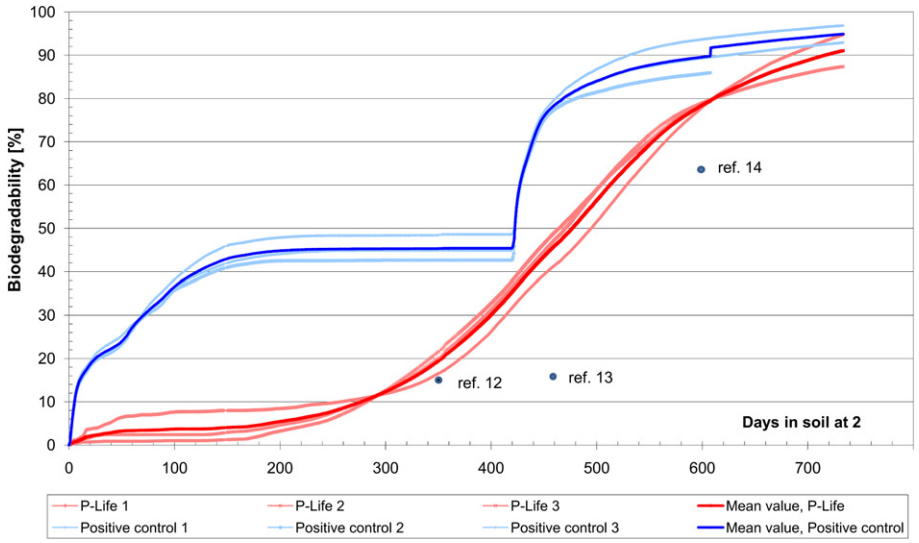

Fig. 3. Mineralization profiles of thermally oxidized test material (red/lower curves) and reference material (blue/upper curves) in the soil test at 23 °C.

where t is exposure time, E_a is activation energy, T is temperature and R is the universal gas constant.

A plot of ln t vs. $1/T$ normally gives straight lines with the slope E_a/R if the Arrhenius relationship is valid. The slope of the lines is a measure of the activation energy (E_a) for the degradation process.

Fig. 2 demonstrates that different activation energies E_a are obtained using the two threshold values as described above. For the THV50, the activation energy was determined to be 84 kJ/mol while the corresponding value for the THV5 was 69 kJ/mol using experimental data from the three highest temperatures. It is also shown that the early stage of oxidation represented by the THV50 curve in Fig. 2 follows linear extrapolation from 75 °C down to room temperature, except for the value obtained at 40 °C, which is probably an artefact. This result is interesting because it overthrows the theory that there is a critical minimum temperature (30 °C) required to initiate the degradation process [18].

On the other hand, non-Arrhenius behaviour (curvature) is demonstrated using THV5 as the criterion. It is well known that degradation of PE is caused by a number of different reactions. In the early stage of oxidation, hydroperoxides are formed and decomposed to alkoxy and hydroxyl radicals. This reaction requires considerable activation energy, thus the rate increases with increasing temperature and is further accelerated by prodegradants. When material is heavily oxidized, many other reactions occur simultaneously, including termination reactions, which is a plausible explanation for the non-Arrhenius behaviour.

In the previous study [15], the activation energy was determined to be 106 kJ/mol using LDPE and another prodegradant system based on a manganese salt. It is apparent from these results that it is necessary to determine the activation energy for each individual material because this energy can vary significantly depending on the formulation and on the endpoint criterion. Consideration must also be given to the possibility of different factors that might cause the degradation process to deviate from the projected straight line, as is demonstrated in Fig. 2 by the THV5 curve. It is evident that the dependence is not linear and despite the fact that the function representing the real kinetics is not known it is also clear that the best fit to all of the experimental data of THV5 is in fact obtained by using a second degree polynomial (see Fig. 2).

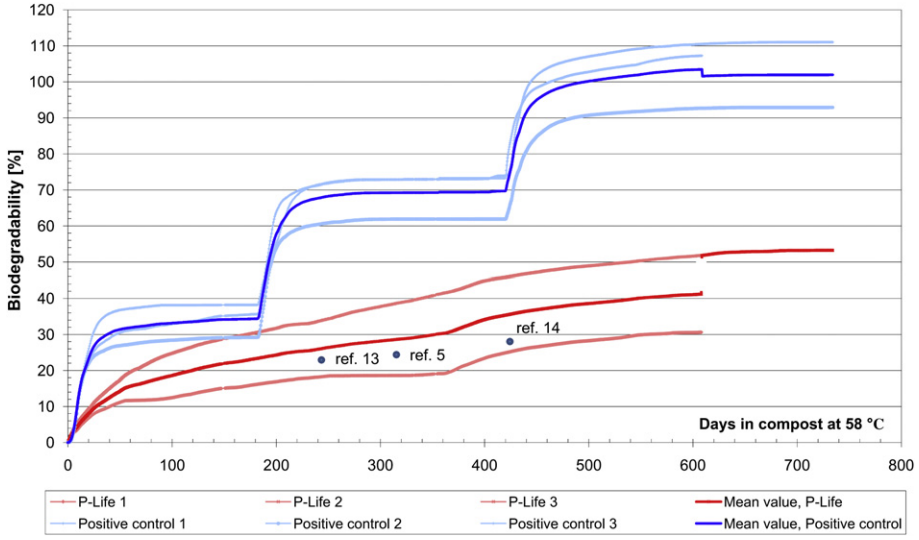

Fig. 4. Mineralization profiles of thermally oxidized test material (red/lower curves) and reference material (blue/upper curves) in the compost test at 58 °C.

3.2. Biodegradation in soil environment

A mineralization test in soil was conducted using thermally pre-oxidized material. A sufficient amount of the film was placed in a heating cabinet for 240 h (10 days) at 65 °C. After this exposure, the weight average molar mass M_w dropped to 8800 and the carbon content to 79%. The molecular weight values of the new and the pre-oxidized materials are given in Table 1 below.

The oxidized material/soil ratio used in the soil biodegradation test was 29 mg/g soil mixture, but if we exclude the Vermiculite, the ratio was 42 mg/g mature compost and plant soil. The accumulated net amount of CO_2 from the test material and the reference material, expressed as a percentage of the maximum theoretical value, is presented in Fig. 3. The mean values of the test material and the reference material are based on three replicates each until 607 days of mineralization. After this period, one vessel containing the test material and one vessel containing the reference material were removed for the subsequent analyses of microbial communities. Consequently, the mean values after 607 days are calculated using the remaining two replicates of each environment.

As demonstrated in Fig. 3, the mineralization curves from the soil experiment may be described by S-shaped curves showing four plain phases. The first phase is characterized by a very low rate of bioassimilation exhibiting about 5% biodegradability after about 180 days. This phase is often referred to as the induction period in the field of reaction kinetics or as the "lag phase" in biodegradation studies. The origin of this phase is usually explained as the time taken for the microbial population to "adapt" to the new material, or substrate. For the definition, standard ISO 14855 can be used.

The second phase is exponential and ranges from 180 to 360 days of mineralization. During this period, the level of biodegradation increases from 5 to about 20–22%. The third phase is the "classical" rate-controlling step with linear increase of biodegradability. After 560 days, the saturation portion starts, but even after 733 days and 91% biodegradability, the process is still in progress. These results are up to 600 days of mineralization in very good agreement with the results obtained by Chiellini et al. [14], who also obtained a plateau at about 4–7% mineralization during about 200 days and thereafter a significant increase in the rate of biodegradation, reaching 63% biodegradation after 600 days and still increasing. They added some water and fresh soil inoculum after five months of incubation and ascribed the subsequent increase in the rate and extent of mineralization to this step. However, in our test, only deionized water was added occasionally to keep the water content constant. Nevertheless, a very similar course of degradation was achieved and an even higher rate of mineralization, thus indicating that reinoculation of the soil mixture is not a necessary condition.

3.3. Biodegradation in compost environment

A mineralization test in the compost at 58 °C was conducted using thermally pre-oxidized material with exactly the same description as in the soil test. However, the mineralization curves from the composting experiment exhibit a different course compared with the soil experiment (see Fig. 4). During the introductory eight weeks, the rate of biodegradation was relatively high. After that, the rate was reduced, exhibiting an almost linear increase of biodegradability with exposure time but at a lower rate. After 470 days, the rate of biodegradation was reduced even more, reaching about 43% mineralization after 607 days. The mean values of the test material are based on two replicates only, and the mean values of the reference material are based on three replicates until 607 days of mineralization. After this period, one vessel containing test material and one vessel containing reference material were removed for the subsequent analyses of microbial communities. Consequently, only one vessel containing test material remained in the test for up to two years while the mean values of the reference material after 607 days are calculated using two replicates. The mineralization profile of the remaining test material did not change significantly during the last period between 607 days and two years (biodegradability increased by only 1%). The mineralization curve of the reference material is composed of three parts. Each part represents mineralization of one portion of the reference material. When the first portion was totally mineralized, an equal portion was added and

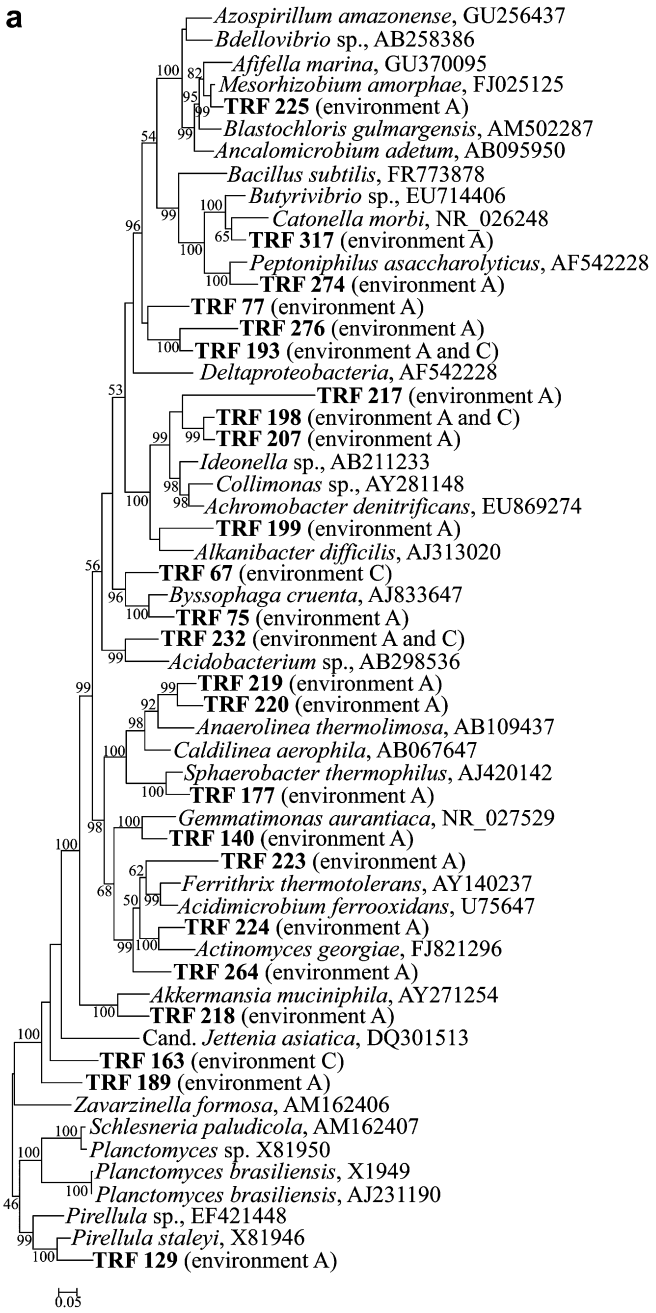

Fig. 5. Maximum-likelihood trees that were linked to specific TRFs in the community profile. The TRF size assigned to each cloned sequence corresponds to TRF numbers in Fig. 6 and the text within the brackets (e.g. "lib"..) shows in which clone library the sequences were retrieved. Bootstrap values >50% (1000 resamplings) are indicated at the nodes. 5a. Using the bacterial 16S rRNA genes (~900 bp) from 24 clones. 5b. Using the archaeal 16S rRNA genes (~600 bp) from 2 clones. 5c. Using the ITS-5.8S DNA region (~700 bp) from 10 clones.

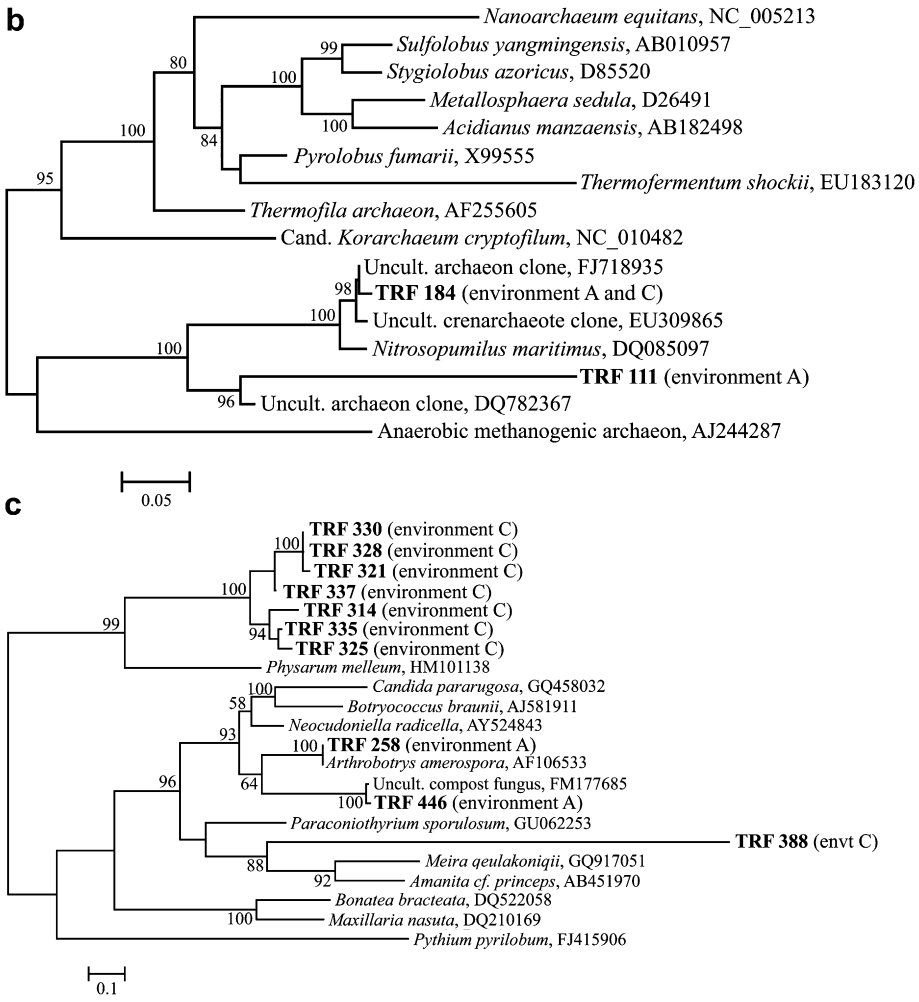

Fig. 5. (*continued*).

when this was assimilated the third portion was added. The mineralization degree of all three portions of the reference material calculated together reached 100% as shown in Fig. 4.

The course of the mineralization curves from our composting experiments is not in agreement with Chiellini et al. [10], who obtained curves from composting (at 55 °C) comparable to the curves from the soil burial test. There are some differences between the two experiments, such as lower temperature and reinoculation with mature compost mixed with fresh soil that were applied by Chiellini et al., which could be responsible for the differences. On the other hand, a close similarity can be seen between the mineralization curves obtained in the present investigation and the previous investigation [15] using different materials.

Despite the differences in the course of compost mineralization, significantly higher levels of biodegradability were obtained in soil compared with compost in both studies. In our study, we obtained 79% biodegradability in soil compared with 43% in compost after 607 days, while Chiellini et al. obtained about 48% in the best run in soil compared with about 26% in compost after 425 days. This result has an important implication because there is a general belief that the rate of mineralization in compost should be higher than in soil because of the difference in temperature. This belief is demonstrated in CEN/TR 15822, where it is proposed to perform "a supplementary test: an accelerated mineralization test method (e.g., EN ISO 14855 performed at 58 °C)". Obviously, the test in compost will create the reverse effect.

3.4. Analysis of microbial communities

The pH in various environments was measured after 180 days and after 606 days of the mineralization test. These values have been used to check whether the pH has contributed to the differences in community composition between the environments. The results of the pH measurements are summarized in Table 2.

3.4.1. Microbial community fingerprints

The T-RFLP profiles of DNA from four different environments after 607 days of mineralization have been established. The following environments were considered: Soil containing residues of the test material (environment A). Soil containing residues of the reference material (environment B). Compost containing residues of the test material (environment C). Compost containing residues of the reference material (environment D).

Table 2
pH measurements in various environments.

	Test material	Reference material	Blank
Soil at start	7.5	7.5	7.5
Soil after 180 days	7.2	7.4	7.2
Soil after 606 days	7.7	7.5	7.4
Compost at start	7.9	7.9	7.9
Compost after 180 days	6.5	6.9	6.6
Compost after 606 days	6.6	7.0	6.9

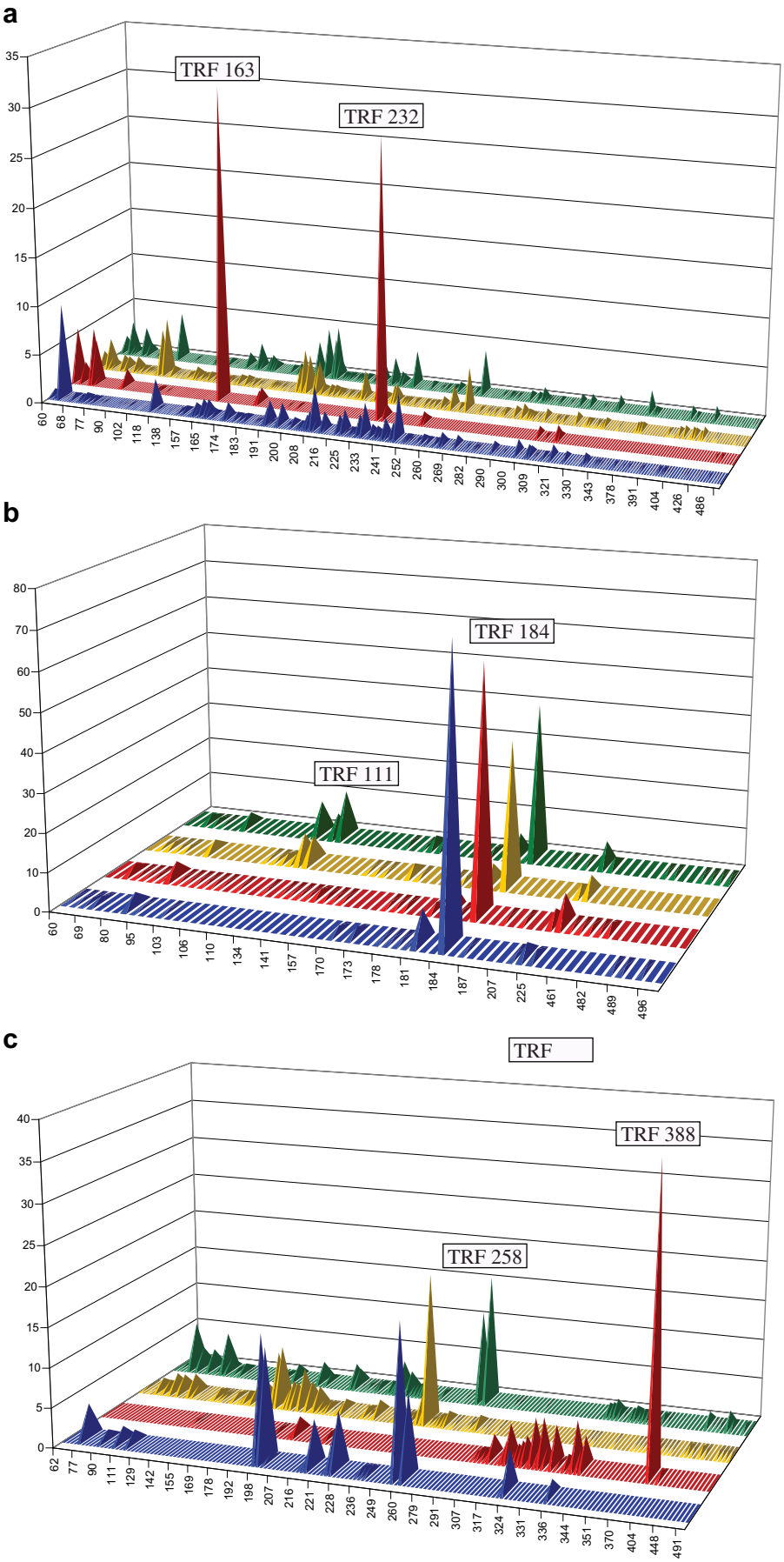

Fig. 6. Relative abundance values for TRFs. Peaks represent the microbial communities as follows: green peaks represent environment A, yellow peaks represent environment B, red peaks represent environment C and blue peaks represent environment D. 6a. dominant bacterial communities obtained using universal bacterial primers and HaeIII restriction digestion. 6b. dominant archaeal communities obtained using universal archaeal primers and TaqI restriction digestion. 6c. dominant fungal communities obtained using universal fungal primers and MaeII restriction digestion.

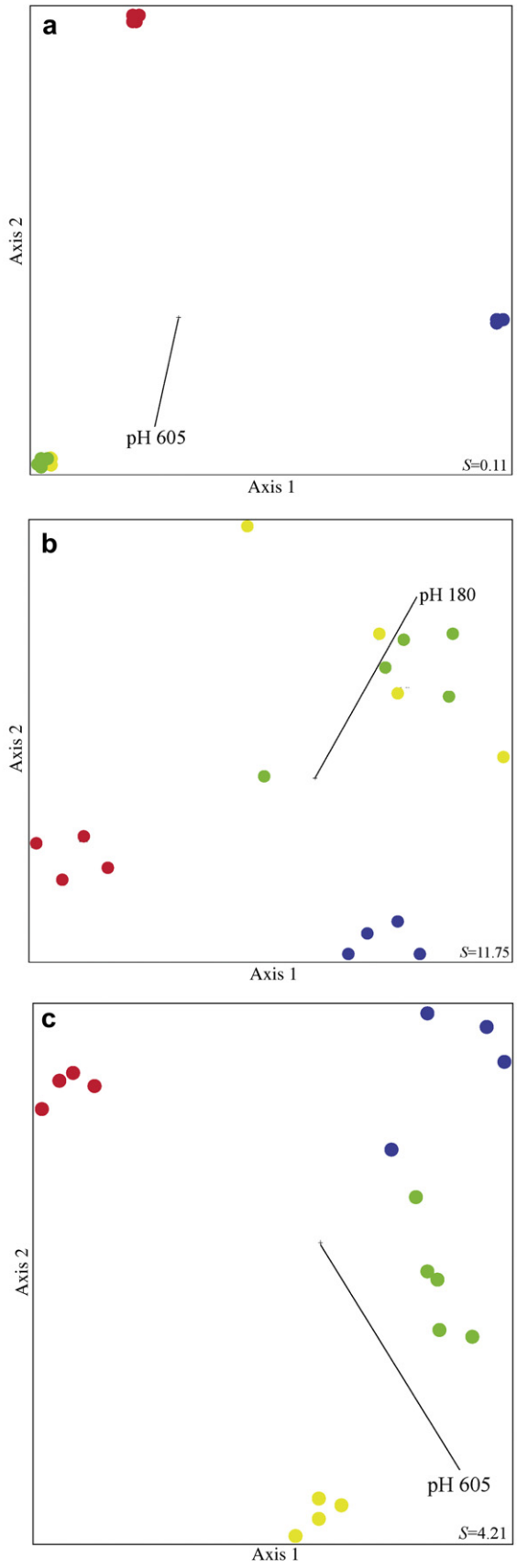

Fig. 7. Non-metric multidimensional scaling ordination from T-RFLP fingerprints in samples from environment A - green circles, environment B - yellow circles, environment C - red circles and environment D - blue circles. pH (as specified in Table 2) correlating to the ordination with $r^2 > 0.5$ are visualized as a vector. Stress values represent the goodness of fit of the regression and are calculated from the differences between distances based on the ordination and those predicted by the regression, respectively. 7a. T-RFLP of the bacterial 16S rRNA gene. (Vector scaling: 50%). (Stress value = 0.11; $P < 0.02$ with 50 permutations by Monte Carlo simulations). 7b. T-RFLP of the archaeal 16S rRNA gene. (Vector scaling: 100%). (Stress value = 11.75; $P < 0.02$ with 50 permutations by Monte Carlo simulations). 7c. T-RFLP of the fungal ITS-5.8S DNA region. (Vector scaling: 100%). (Stress value = 4.21; $P < 0.02$ with 50 permutations by Monte Carlo simulations).

The T-RFLP profiles of DNA from compost and soil microbial communities showed clear differences between the environments (Figs. 6 and 7). Samples from different environments clustered apart for all of the microbial groups (i.e., bacteria, archaea and fungi), except for the archaea in the soil samples (environments A and B) (Fig. 7b). For example, the bacterial community composition varied dramatically between compost amended with the reference material and compost containing the test material, indicating a structural shift coupled to the test material. The same was also true for fungal communities. Probably, these differences in microbial community composition resulting from the addition of the test material can be linked to the different functional traits of this specific environment. The compost samples were more similar to each other regarding archaea and fungi in comparison with those from the soil system, which presented larger internal variations. For the bacterial communities, almost no internal variation in the samples from the different environments was seen (Fig. 7a). The ranking showed correlations with pH, indicating that pH might be one explanation for the differences in community structure between the environments (Fig. 7). Consistently, the Mantel test showed correlations between the differences in bacterial community structure among the samples and dissimilarities in pH ($r = 0.73$, $P < 0.001$), as well as for the archaeal community structure ($r = 0.61$, $P < 0.001$) and the fungal community ($r = 0.65$, $P < 0.001$).

3.4.2. *Identification of specific TRFs*

The different environments among the bacterial and fungal profiles exhibited fairly different T-RFLP patterns (Fig. 6), whereas the archaeal community composition was much the same in all environments. In particular, TRFs from environment C, dominated by two bacterial TRFs, viz., TRF 163 and TRF 232, and one fungal, viz., TRF 388 were entirely divergent compared with the other environments. TRF 163, representing one of the most dominant peaks within the bacterial profile in environment C (Fig. 6a), was most directly linked to an uncultured bacterial clone, whereas TRF 388, the most dominant peak in the fungal community from environment C, seemed to be related to *Meira* and *Amanita* spp and to *Paraconyothyrium sporulosum*, which has been identified as manganese-oxidizing fungi [19] (Fig. 6c). The most dominant TRF within the archaeal community profiles, TRF 184 (Fig. 6b) was linked to uncultured archaeon clones and *Nitrosopumilus maritimus* (Fig. 5b). The microbial identities ascribed to the rest of the TRFs representing the main differences between the community profiles of the different environments (TRFs 232, 258 and 111 in Figs. 5 and 6) belonged to various genera and classes, as concluded from maximum-likelihood trees (Fig. 5). Overall, the majority of cloned sequences were identified as uncultured and uncharacterized microorganisms, whereas a large proportion of the less dominant TRFs in the profiles could not be linked to a sequence.

4. Conclusions

Biodegradable polymers exhibit a delicate balance between the achievement of useful technological performance and rapid and

effective biodegradability. It is therefore important to estimate reliably the useful lifetime of a material. For such an estimation, it is necessary to determine the activation energy for each individual material because this energy can vary significantly depending on the formulation, as has been shown in this investigation. If two different materials have a lifetime of one week at 70 °C, the predicted lifetime at 23 °C will be about two years for the material with an activation energy of 84 kJ/mol (as was found in this investigation) or seven years if the material has an activation energy of 106 kJ/mol, as was found in the previous study [15]. It has also been demonstrated that when the material is heavily oxidized, non-Arrhenius behaviour (curvature) is observed instead of linear extrapolation in the abiotic degradation studies.

Results obtained after two years of biodegradation experiments have shown significantly higher levels of biodegradability in the soil environment at 23 °C compared with the compost environment at 58 °C. After two years in the soil mineralization experiment, 91% biodegradability was achieved without reaching a plateau phase. This result has two important implications. The most important one is that it is possible to create LDPE-based materials that will almost completely biodegrade in soil within two years. It also indicates that the risk of plastic fragments remaining in soil indefinitely is very low. The second important implication is that carbon from the oxidized PE is to an overwhelming extent converted to carbon dioxide in the soil mineralization and only to a small extent converted to new biomass.

The much higher rate of mineralization of the oxidized PE in soil at 23 °C compared with composting at 58 °C gave rise to a study of divergences in microbial communities between these two environments. It has been found that the most dominant bacterial and fungal TRFs in the compost containing the test material are totally different from the three other environments. In particular, it is interesting to note a great difference between compost containing the test material and that containing the reference material, which indicates that the presence of the test material favours growth of a few special microbial species. Finding that the most dominant fungal TRF 388 in the compost containing the test material is closely related to *P. sporulosum*, which has been identified as manganese-oxidizing fungi, is also very interesting as this could partially explain the low rate of biodegradation in this environment.

Acknowledgments

The authors are grateful to P-Life Japan Inc. for financial support and valuable discussions. Many thanks to Ms. Linda Eriksson, Mrs. Susanne Ekendahl and Mrs. Catrin Lindblad for the persistent work with the biodegradability tests.

References

[1] Scott G. Polym Age 1975;6:54.
[2] Albertsson AC. Pure Appl Chem 1993;A30(9&10):757.
[3] Singh B, Sharma N. Polym Degrad Stab 2008;93:561–84.
[4] Celina M, Gillen KT, Assink RA. Polym Degrad Stab 2005;90:395–404.
[5] Fontanella S, Bonhomme S, Koutny M, Husarova L, Brusson J-M, Courdavault J-P. Polym Degrad Stab 2010;95:1011–21.
[6] Roy PK, Titus S, Surekha P, Tulsi E, Deshmukh C, Rajagopal C. Polym Degrad Stab 2008;93:1917–22.
[7] Kershaw MJ, Talbot NJ. Fungal Genet Biol 1998;23:18–33.
[8] Seneviratne G, Tennakoon NS, Weerasekara MLMAW, Nandasena KA. Curr Sci 2006;90:20–1.
[9] Corti A, Muniyasamy S, Vitali M, Imam SH, Chiellini E. Polym Degrad Stab 2010;95:1006–114.
[10] Zahra S, Abbas SS, Mahsa M-T, Mahsen N. Waste Manage 2010;30:396–401.
[11] Chiellini E, Corti A, D'Antone S, Billingham NC. J Polym Environ 2007;15 (3):169–78.
[12] Thomas N, Clarke J , McLauchlin A, Patrick S. EV0422. Department for Environment, Food and Rural Affairs (DEFRA); January 2010.
[13] Husarova L, Machovsky M, Gerych P, Houser J, Koutny M. Polym Degrad Stab 2010;95:1794–9.
[14] Chiellini E, Corti A, Swift G. Polym Degrad Stab 2003;81:341–51.
[15] Jakubowicz I. Polym Degrad Stab 2003;80:39–43.
[16] Muyzer G, de Waal EC, Uitterlinden AG. Appl Environ Microbiol 1993;59:695–700.
[17] Weisburg WG, Barns SM, Pelletier DA, Lane DJ. J Bacteriol 1991;173:697–703.
[18] Carter MJ. Assessment of the physical degradation in a landfill environment of plastics manufactured with TDPA. EPI/RES/JHP/2209/01a; 2002. 1–13.
[19] Takano K, Itoh Y, Ogino T, Kurosawa K, Sasaki K. Limnology December 2006;7:219–23.
[20] Baker GC, Smith JJ, Cowan DA. J Microbiol Methods 2003;55:541–55.
[21] White TJ, Burns T, Lee S, Taylor J. In: Innis MA, editor. PCR protocols. A guide to methods and applications. San Diego: Academic Press; 1990. p. 315–22.
[22] Kaiser HF. Psychometrika 1958;23:187–200.
[23] Mantel N. Cancer Res 1967;27:209–20.